Growth rate of nonthermodynamic emittance of intense electron beams

Bruce E. Carlsten
Los Alamos National Laboratory, Los Alamos, New Mexico 87545
(Received 25 November 1997)

The nonlinear free-energy concept has been particularly useful in estimating the emittance growth resulting from any excess energy of electron beams in periodic and uniform channels. However, additional emittance growth, that is geometrical rather than thermodynamic in origin, is induced if the particles have different kinetic energies and axial velocities, which is common for mildly relativistic, very intense electron beams. This effect is especially strong if particles lose or gain significant kinetic energy due to the beam's potential depression, as the beam converges and diverges. In this paper we analyze these geometric emittance growth mechanisms for a uniform, continuous, intense electron beam in a focusing transport channel consisting of discrete solenoidal magnets, over distances short enough that the beam does not reach equilibrium. These emittance growth mechanisms are based on the effects of (1) energy variations leading to nonlinearities in the space-charge force even if the current density is uniform, (2) an axial velocity shear radially along the beam due to the beam's azimuthal motion in the solenoids, and (3) an energy redistribution of the beam as the beam compresses or expands. The geometric emittance growth is compared in magnitude with that resulting from the nonlinear free energy, for the case of a mismatched beam in a uniform channel, and is shown to dominate for certain experimental conditions. Rules for minimizing the emittance along a beamline are outlined.
[S1063-651X(98)01108-8]

PACS number(s): 41.75.Ht, 03.50.De, 29.27.Bd

I. INTRODUCTION

In this paper we will analyze some dominant emittance growth mechanisms of a continuous, intense electron beam in a transport channel made up of short discrete solenoids, where the normalized, rms emittance is defined by

$$\varepsilon = \gamma\beta\sqrt{\langle r^2\rangle\langle r'^2\rangle - \langle rr'\rangle^2}/2, \tag{1}$$

γ is the relativistic mass factor, β is the axial velocity normalized to the speed of light, the prime refers to an axial derivative, and the brackets indicate ensemble averages. Although the emittance defined this way is not strictly conserved (if the beam has a nonzero energy spread and either is accelerated or experiences linear focusing), it is a practical, geometrical definition, because it relates the emittance to the minimum rms beam size achievable for a drifting beam at a waist or target position. We will assume that the transport channel is short with a few discrete focusing elements, the focusing is not necessarily periodic, and the electron beam does not reach an equilibrium or periodic phase-space distribution. For simplicity in the analytic treatment, we will assume that the beam is laminar with uniform density, and all focusing elements are perfect with no fringe fields or misalignments, which eliminates several very significant emittance growth mechanisms, such as the corkscrew mechanism [1–3] and radial aberrations in the focusing. The mechanisms we will study here are based on kinetic energy and axial velocity variations of the particles in the beam. These variations will lead to an increase in the geometrical emittance, as defined by Eq. (1), but will not lead to an associated increase in the beam's entropy. Since these effects are not thermodynamic in nature, they are not included in standard analyses of the nonlinear free-energy mechanism [4–6]. The most important of these mechanism results from particles gaining and losing kinetic energy as the beam compresses and expands, from the beam's own potential depression. Even if the applied forces are linear [specifically $d(\gamma\dot{r})/dt$ for each particle is linear in radius, where the dot refers to a time derivative], variations in the kinetic energies and axial velocities of the particles will lead to effective nonlinear terms in the radial equation of motion where the axial coordinate is used (specifically dr'/dz for each particle will not be proportional to the particle's radius). These mechanisms, which have been previously largely ignored, are becoming important for a new, emerging generation of high-current, low-emittance induction linear accelerators, and are the focus of this paper. The emittance growth described in this paper is essentially geometric in nature, and is not related to the thermodynamic energy of the beam. Since this emittance growth results from energy variations, it could also be referred to as a chromatic emittance growth, but we choose the term geometric because the growth arises from using the geometric emittance definition, Eq. (1), instead of using the emittance defined by the ensemble averages of the conjugate variables r and $\gamma\dot{r}$. Additionally, we do not want these mechanisms confused with the chromatic effects resulting from the energy spread that exists axially along a finite-length bunch. In regards to recent discussions relating beam emittance to entropy [7,8], the emittance growth described by the nonlinear free energy is related to a real increase in entropy, whereas the emittance growth resulting from the geometrical effects studied here is not related to a real increase in entropy. In this manner, this type of emittance growth is similar to the nonequilibrium emittance growth seen in photoinjectors, which can be compensated [9–13], leading to an emittance that initially grows and then decreases to a final equilibrium value often between a fourth and a tenth of the maximum emittance. The nonequilibrium emittance in photoinjectors is axial in nature due to the pulsed nature of the bunched beam;

the geometric emittance studied in this paper is radial in nature because the beam is continuous.

Much of the previous work on the emittance growth of electron beams in focusing channels [4–6] has concentrated on the powerful approach of the evolution of nonlinear free energy. This concept is based on the fact that stationary states of the channel (using either periodic or uniform focusing) are minimum-energy states (for given second moments of the beam, including its rms emittance). Thus a beam in a nonstationary distribution state will have a higher energy per particle than the equivalent stationary state, and will try to relax to the stationary state with that amount of average energy per particle. The higher-energy stationary state will have larger second moments, including the rms emittance, than the initial distribution. This relaxation will be triggered by any nonlinear forces present; beam density nonuniformities typically relax in about a quarter-plasma period, and beam mismatches or transverse offsets typically relax with distances on the order of the betatron motion. The energy conservation leading to this effect exists because the stationary states are eigenstates of the Hamiltonian of the system. Strictly, this conservation property only exists for the Hamiltonian conjugate variables r and $\gamma\dot{r}$. The beam rms emittance is typically defined with the variables r and r'; thus an equivalent conservation property for the rms emittance growth also exists for these variables if all particles are assumed to have the same energy and axial velocity. However, for intense electron beams, this assumption fails, as we demonstrate in this paper. The result is that there can be a nonthermodynamic increase in the beam's rms emittance, which is not related to the particles' average energy. It could be argued that this then is not a real emittance increase; however, the normalized rms emittance as defined in Eq. (1) will increase, as will the minimum achievable rms waist radius as the beam is focused.

Here, we will carefully expand the relativistic radial equation of motion for a uniform-density, laminar electron beam, and find that several nonlinear terms arise from the variations in the particles' energies. In fact, even though the beam distribution is uniform and the space-charge force is radially linear, these other terms can lead to emittance growths that accumulate along the beamline. The mechanisms that have the largest emittance growth rates result from energy fluctuations due to the particles' radial motion and axial velocity variations due to the particles' azimuthal motion within the solenoids. These mechanisms can lead to very significant emittance growth rates for initially low-emittance beams with uniform densities; the normalized emittance growth rates due to these mechanisms also do not necessarily decrease with increasing beam energy, unlike that arising from the space-charge force if the beam density is nonuniform. Thus the emittance growths discussed in this paper are of very practical concern for low-emittance, high-current, relativistic accelerators, where special care has been taken to design an electron gun producing a uniform-density beam. One goal of this paper is to develop formulas that can be used by induction-accelerator beamline designers as a figure of merit. This formalism does not assume uniform or periodic focusing, and can be used to estimate the emittance growth of electron beams in nonperiodic focusing structures where no equilibrium beam distribution exists, as seen in many existing and proposed beamlines. Using numerical simulations, we additionally demonstrate that these mechanisms also lead to the beam density hollowing out.

We will start by constructing the radial equation of motion including the effect of both the space-charge force and the focusing force from a perfect, hard-edged solenoid. Then, we will examine the emittance growth for the effects outlined above, making the assumption that the emittance growth is primarily due to changes in the particles' radial velocities and that the beam density profile essentially remains constant. Although this procedure does not lead to a self-consistent beam stationary state solution, this procedure is common for estimating emittance growth rates of nonequilibrium electron beams (see Refs. [12,14], for example) and will lead to insights into the emittance growth mechanisms. Finally we will compare the emittance growth from a mismatched beam from this effect with that estimated by the nonlinear free energy, and demonstrate that for sufficiently intense, relativistic, low-emittance electron beams, the effect from the energy variations will dominate.

II. DERIVATION OF THE RADIAL EQUATION OF MOTION, INCLUDING NONLINEAR FOCUSING FORCES

In this section we wish to derive an expression for the radial equation of motion that we can use to examine various emittance growth mechanisms. In particular, we wish to have an expression we can use to estimate the emittance growth for a laminar, uniform-density beam.

We will consider the radial equation of motion for a particle, and to expand the force terms for a specific particle around the force seen by a nominal particle at the beam's center. We will then assume that each particle experiences a constant force over some axial distance l as they drift. Once this is done, the emittance growth can be easily evaluated by performing the ensemble averages in Eq. (1), since we are assuming that the radial current density remains constant. This approach will not deal with correlations in the emittance growth relative to the initial distribution. Since we are interested in the emittance growth from nonlinear components of the space-charge and focusing forces, we will expand the radial equation of motion carefully.

Radial force equation

The radial equation of motion for a particle within the beam within the central part of a solenoid (where the applied magnetic field from the solenoid is purely axial) is given by

$$m\frac{d(\gamma\dot{r})}{dt}=eE_r+e(v_\theta B_{\rm dia}-v_z B_\theta)+ev_\theta B_{\rm ext}+\frac{\gamma m v_\theta^2}{r}, \tag{2}$$

where $B_{\rm ext}$ is the total external axial magnetic field (from both the solenoid and the diamagnetic effect from the image currents in the beampipe), $B_{\rm dia}$ is the induced diamagnetic axial magnetic field from the beam current opposing the solenoidal field, B_θ is the azimuthal magnetic field from the space charge, and E_r is the radial electric field from the space charge, all at the position of the particle, and e and m are the electronic charge and mass, respectively. Most of

these terms are mostly linear with radius. For balanced flow (the beam edge is at a constant radius), the linear components cancel. The $v_z B_\theta$ term mostly cancels E_r (to order $1/\gamma^2$). For balanced flow, the solenoid strength is adjusted such that the linear part of the combination of $ev_\theta B_{\rm ext}$ and the centrifugal force will cancel the linear part of the resulting space-charge force. There is also a potential depression within the beam (a variation of γ that is a function of radius). Our approach will be to expand the radial equation of motion in terms of the variation of γ, to lowest order, which we will then use to estimate the emittance growth for various cases.

We will assume that the particles have no intrinsic angular momentum (there is no axial magnetic field at the location of the cathode) and that the external magnetic field is radially constant. Thus the azimuthal velocity can found by application of Busch's theorem [15] (the conservation of angular momentum):

$$v_\theta = -\frac{e}{\gamma m r}\int_0^r (B_{\rm ext}+B_{\rm dia})\,\nu\,d\nu, \tag{3}$$

where ν is a dummy variable for the radial integration. We will assume that any radial divergence of the beam is small, and use Gauss's law to find the radial electric field,

$$E_r(r) = \int_0^r \frac{\rho(\nu)\,\nu}{\varepsilon r}\,d\nu, \tag{4}$$

where ρ is the charge density. The diamagnetic field is given by

$$B_{\rm dia} = \int_r^{r_b} \mu v_\theta(\nu)\rho(\nu)d\nu, \tag{5}$$

where r_b is the radial edge of the beam. The diamagnetic field is small, and, to first order, only the azimuthal velocity depending on the externally applied solenoidal field needs to be considered in Eq. (5). The relativistic mass factor is given by

$$\gamma(r) = \gamma_a + \gamma_1(r) = \gamma_a + \int_0^r \frac{eE_r(\nu)}{mc^2}\,d\nu, \tag{6}$$

where γ_a is the mass factor along the axis ($r=0$). Let us assume that the space-charge density is of the form $\rho = \rho_0 r^n$. Explicit evaluation of the above integrals for this charge density profile gives

$$E_r = \frac{\rho_0}{\varepsilon(n+2)}\,r^{n+1},$$

$$\gamma_1 = \frac{e}{mc^2}\frac{\rho_0}{\varepsilon(n+2)^2}\,r^{n+2} = \frac{eE_r}{mc^2}\frac{r}{n+2},$$

$$\frac{B_{\rm dia}}{B_{\rm ext}} = -\frac{\mu e}{2m\gamma}\frac{\rho_0}{(n+2)}(r_b^{n+2}-r^{n+2}) = -\left(\frac{\gamma_b}{\gamma_a}-\frac{\gamma_1}{\gamma_a}\right)\frac{n+2}{2}, \tag{7}$$

where we have now introduced γ_b as the difference in the relativistic mass factor between the center and the radial edge of the beam. We can manipulate the axial field components in order to find a more useful form. The total magnetic field B in terms of the diamagnetic component and the total externally applied field $B_{\rm ext}$ is given to lowest order by

$$B = B_{\rm ext}\left(1+\frac{B_{\rm dia}}{B_{\rm ext}}\right) = B_{\rm ext}\left[1-\frac{\gamma_b}{\gamma_a}\left(\frac{n+2}{2}\right)+\frac{\gamma_1}{\gamma_a}\left(\frac{n+2}{2}\right)\right]$$
$$= B_a\left[1+\frac{\gamma_1}{\gamma_a}\left(\frac{n+2}{2}\right)\right], \tag{8}$$

where B_a is the total axial magnetic field along the axis ($r=0$). If the charge density is uniform ($n=0$), the total axial magnetic field and the relativistic mass factor have the same radial dependency,

$$B = B_a\left(1+\frac{\gamma_1}{\gamma_a}\right),$$

$$\gamma = \gamma_a\left(1+\frac{\gamma_1}{\gamma_a}\right). \tag{9}$$

Note that γ_1 depends quadratically on the beam radius, and is positive [see Eq. (7)].

The azimuthal velocity in terms of the magnetic field on axis and the relativistic mass factor on axis is given by

$$v_\theta = -\frac{eB_a r}{2\gamma_a m}\left(\frac{1+(\gamma_1/\gamma_a)(n+2)/(n+4)}{1+\gamma_1/\gamma_a}\right). \tag{10}$$

Note that the azimuthal velocity is not radially linear even if the space-charge density is uniform ($n=0$).

The beam-induced azimuthal magnetic field in Eq. (2) is given in terms of the vector potential by

$$B_\theta = \frac{\partial}{\partial z}A_r + \frac{1}{r}\frac{\partial}{\partial r}rA_z. \tag{11}$$

If the beam is converging or diverging, there is a nonzero radial vector potential, and if the beam is being focused in a solenoid, the axial derivative of the radial vector potential is nonzero [16]. The term corresponding to the axial derivative of the radial vector potential tends to average out for a laminar beam and will not result in an appreciable emittance growth, and we will ignore it.

At this point, we have written out all the terms on the right-hand side of the radial equation of motion, and we can evaluate the nonlinear terms. For the emittance analysis, we want the radial divergence instead of the radial velocity, so we still need to change the variable of differentiation on the left-hand side of the radial equation of motion. (This change of variable is what induces the geometric emittance growth.) Using dots to refer to time derivatives and primes to refer to axial derivatives, we have

$$\frac{d}{dt}\gamma\dot r = \dot r\frac{d\gamma}{dt}+\gamma\ddot r = \frac{eE_r}{mc^2}\dot r^2+\gamma\ddot r. \tag{12}$$

With the definitions v_a being the axial velocity along the axis and v being the relative axial velocity,

$$v_z(r) = v_a + v(r), \tag{13}$$

Eq. (2) becomes

$$r''mv_a^2\left(1+2\frac{\nu}{\nu_a}\right)=\frac{eE_r}{\gamma\gamma^*(r)^2}+\frac{1}{\gamma}\left(ev_\theta(B_{\rm ext}+B_{\rm dia})+\frac{\gamma m v_\theta^2}{r}\right)-\frac{e}{c^2\gamma}v_0^2E_r r'^2, \tag{14}$$

where γ^* is an effective relativistic mass factor we will evaluate later. To lowest order in the small quantities, the radial force equation becomes in terms of the parameters evaluated on axis

$$r''=\left[\frac{eE_r}{mv_a^2\gamma_a\gamma^*(r)^2}\left(1-\frac{\gamma_1}{\gamma_a}\right)-\frac{e^2B_a^2r}{4\gamma_a^2m^2v_a^2}\left(1+n\frac{\gamma_1}{\gamma_a}\right)-\frac{eE_r r'^2}{\gamma_a mc^2}\right]\left(1-2\frac{v}{v_a}\right). \tag{15}$$

The focal length of a solenoid of length l for the beam near the axis is defined by

$$f=\frac{4\gamma_a^2m^2v_a^2}{le^2B_a^2} \tag{16}$$

and so the change in the radial divergence after a length l becomes

$$\delta r'=\left[\frac{leE_r}{m\nu_a^2\gamma_a\gamma^*(r)^2}\left(1-\frac{\gamma_1}{\gamma_a}\right)-\frac{r}{f}\left(1+n\frac{\gamma_1}{\gamma_a}\right)-\frac{leE_r r_0'^2}{\gamma_a mc^2}\right]\left(1-2\frac{v}{v_a}\right), \tag{17}$$

where r_0' is the initial beam divergence.

If the charge density is uniform, the change in the radial divergence becomes

$$\delta r'=\left[\frac{leE_r}{m\nu_a^2\gamma_a\gamma^*(r)^2}\left(1-\frac{\gamma_1}{\gamma_a}\right)-\frac{r}{f}-\frac{le}{\gamma_a mc^2}E_r r_0'^2\right]\left(1-2\frac{v}{v_a}\right). \tag{18}$$

Note that the effect of the potential depression of the beam exactly cancels the effect of the diamagnetic effect, leading to a purely linear focusing force. The apparent nonlinearities in this equation (which governs the emittance growth) are (1) the term modifying the space-charge force, which results from the variations in the different particles' relativistic mass factors, (2) the last term within the square brackets, which results from how the particles' mass factor changes as the beam converges or diverges, and (3) the last term in the final parentheses, which results from variations in the particles' axial velocity. If the emittance is defined by the rms ensemble averages of r and $\gamma\dot{r}$, it would not grow, reflecting the fact that the growth in the emittance defined in the usual way [Eq. (1)] does not reflect a thermodynamic change in the beam distribution.

III. EMITTANCE GROWTH ESTIMATES

In this section we will estimate the emittance growth due to variations in particle energies and axial velocities, for typical focusing scenarios of a uniform-density, laminar beam. We will make the assumption that this emittance growth adds in quadrature with a beam's initial emittance, for a beam with nonzero initial emittance. This assumption really has two parts: (1) the emittance growth for a nonlaminar beam is the same as for a laminar beam and (2) the beam's initial emittance is uncorrelated with the emittance growth. These resulting emittance growths are not derivable from nonlinear free-energy considerations [4–6], but instead arise from geometric nonlinearities in the introduced radial divergence [Eq. (18)]—in particular, from (1) the γ_1/γ_a term multiplying the space-charge force, (2) the $r_0'^2$ term, and (3) the v/v_a term. The emittance growth from (1) is physically due to a nonlinearity in the radial equation of motion because a particle's radial acceleration depends on its relativistic mass, in addition to the space-charge force. The emittance growth from (2) arises from the fact that even if the radial momentum change is linear, if particles at different radii gain or lose energy at different rates, this will lead to a nonlinearity in the radial equation of motion for r'. Because of issue (3), particles at different radii inside a solenoid end up spending a different amount of time experiencing the solenoid's focusing fields (and thus are affected by a different focal length).

We will assume that the focusing elements are thin for simplicity. In the emittance growth formulas that we derive later, the focusing element length is important only for the case of the variation of axial velocities in a solenoid.

The emittance growth from the nonlinear space-charge force term scales as $1/\gamma^3$ (if the density is nonuniform it scales as $1/\gamma^2$). Thus, as the beam is accelerated, the emittance growth from this effect vanishes, and, for most beamlines with acceleration, the net accumulated emittance growth is small. However, the emittance growths from the other effects do not necessarily decrease as the beam is accelerated, and very large net emittance growths can occur, even for beamlines with acceleration. Clearly, the correlations between particle motion and the nonlinear forces will have an important effect on the net emittance growth, which will not be considered beyond some simulation results presented in the following section; however, the emittance growth rates derived in this section still can be used to estimate the emittance growth in beamline designs.

A. Balanced uniform flow

In this section we will assume that the focusing just balances the radial space-charge force near the axis of the beam, and that the initial beam divergence vanishes, $r_0'=0$. In this case, the third term within the first parentheses in Eq. (18) vanishes, and any nonlinearity introduced in the radial divergence comes from the nonlinearity in the first term within the first parentheses (all nonlinear effects from terms within the second parentheses are second order).

Balanced flow means that

$$\frac{leE_r}{v_a^2\gamma_a^3}=\frac{r}{f}=\frac{le^2B_a^2r}{4\gamma_a^2mv_a^2}. \tag{19}$$

There is clearly a nonlinearity in the space-charge force associated with the beam's potential depression, but it is also instructive to investigate the linearity of the γ^* factor in the space-charge term.

The space-charge radial electric field at a radial position r from a ring at radius ν is given by

$$dE_r=\frac{\rho_0\nu}{\varepsilon r}\,d\nu. \tag{20}$$

The radial force at r is then given by

$$F_r(r)=\int_0^r \frac{e\rho_0\nu}{\varepsilon r}\,[1-\beta(r)\beta(\nu)]d\nu, \tag{21}$$

which is easily evaluated as soon as we have an expression for the axial velocity as a function of radial position.

The axial velocity is found from the conservation of energy:

$$1-\beta_z^2-\beta_\theta^2=\frac{1}{\gamma^2}=\frac{1}{\gamma_a^2}\left(1-\frac{2\gamma_1(r)}{\gamma_a}+\frac{3\gamma_1(r)^2}{\gamma_a^2}\right), \tag{22}$$

where, as before, γ_a is the normalized beam energy along the axis and $\gamma_1(r)$ is the beam energy change from the axis, and we have kept this equation to second order in γ_1/γ_a. From before, we know that the azimuthal velocity is given to lowest order by

$$\beta_\theta^2=\left(\frac{eB_ar}{2\gamma_amc}\right)^2=2\frac{\gamma_1}{\gamma_a^3}, \tag{23}$$

using the condition of balanced flow [Eq. (19)] and the relation between the radial electric field and the potential depression for a uniform beam. Using this expression in Eq. (22), we find

$$1-\beta_z^2=\frac{1}{\gamma_a^2}\left(1+\frac{3\gamma_1^2}{\gamma_a^2}\right), \tag{24}$$

and any variation in the axial beam velocity is second order in the small quantities. Thus the entire beam essentially has the same axial velocity, and indeed $\gamma^*=\gamma_a$, to first order in γ_1/γ_a. This is a more general case of the same well-known effect for Brillouin flow for tenuous electron beams [15].

In order to estimate the emittance growth from the nonlinear contribution from the radial space-charge force, we start with the nonlinear part of Eq. (18),

$$\delta r'=-\frac{leE_r\gamma_1}{mv_a^2\gamma_a^4}. \tag{25}$$

In terms of the beam current, the radial electric field is given by

$$E_r=\frac{Ir}{2\pi\varepsilon r_b^2v_a}. \tag{26}$$

Using the definition of the Alfvén current ($I_A=4\pi\varepsilon mc^3/e$), we can rewrite the change in the beam divergence as

$$\delta r'=-2\frac{I^2lr^3}{I_A^2\beta^4\gamma_a^4r_b^4}, \tag{27}$$

where $\beta=v_a/c$. After doing the ensemble averages (recall we are assuming that the initial beam density is uniform), we find that the normalized, 90% emittance is

$$\varepsilon=l\frac{\sqrt{2}I^2}{12\beta^3\gamma_a^3I_A^2}. \tag{28}$$

For a 4-kA beam at 6 MeV (the rough parameters of the Integrated Test Stand (ITS) induction linac at Los Alamos [17]), the emittance growth is about $3.2(10^{-6})l$. Note that this emittance growth is independent of beam radius.

We would not expect that the emittance would grow unbounded at this rate. The beam density will continue to oscillate about the equilibrium density (somewhat lower at the beam edge than at the beam center), with the emittance oscillating also, with a period equal to one-half of the plasma period. For this case, the generalized perveance $K=2I/I_A(\beta\gamma_a)^3$ [6] is 2.3×10^{-4}, and the beam travels a distance $\pi r_b/2\sqrt{2K}=2.2$ m in a quarter-plasma period.

There are three features of this emittance growth we should note. First, this emittance growth is only a function of beam energy and current. Second, it is a small effect, and one that vanishes quickly as the energy is increased. Third, the emittance growth from this effect will oscillate for a laminar beam, and the emittance will vanish at integer multiples of a half-plasma wavelength.

We can verify these conclusions using the relativistic particle-pushing code SLICE [18], which uses the Lorentz force equation along with external fields and the beam's self-fields to calculate particle trajectories. For a balanced, monokinetic-energetic beam that should have no emittance growth according to Eq. (18) (here the beam is injected with equal kinetic energies at all radii, ignoring the potential depression of the beam), the numerical error due to the interpolation of the particles' positions leads to an emittance oscillation that is roughly of the size of $0.35(10^{-3})$ m divided by the number of particles in the simulation [in other words about $0.35(10^{-6})$ m for 1000 simulation particles, which is negligible]. In Fig. 1 we show simulation results for a balanced beam injected with uniform total energy (kinetic plus potential) with the above parameters. The initial emittance growth rate is very close to $2(10^{-6})$ m per meter of drift, and oscillates with a period corresponding to a half-plasma period. Note that the emittance growth results from a differential rotation in phase space, shown in the phase-space plot at the final axial location (28 m) in Fig. 1(c). Close inspection of the phase-space plots at different axial locations shows that this differential rotation changes sign in successive emittance oscillations, and the curvature in the final phase-space plot is of the correct sign. This oscillation is very different than the emittance growth resulting from the nonlinear free energy, in

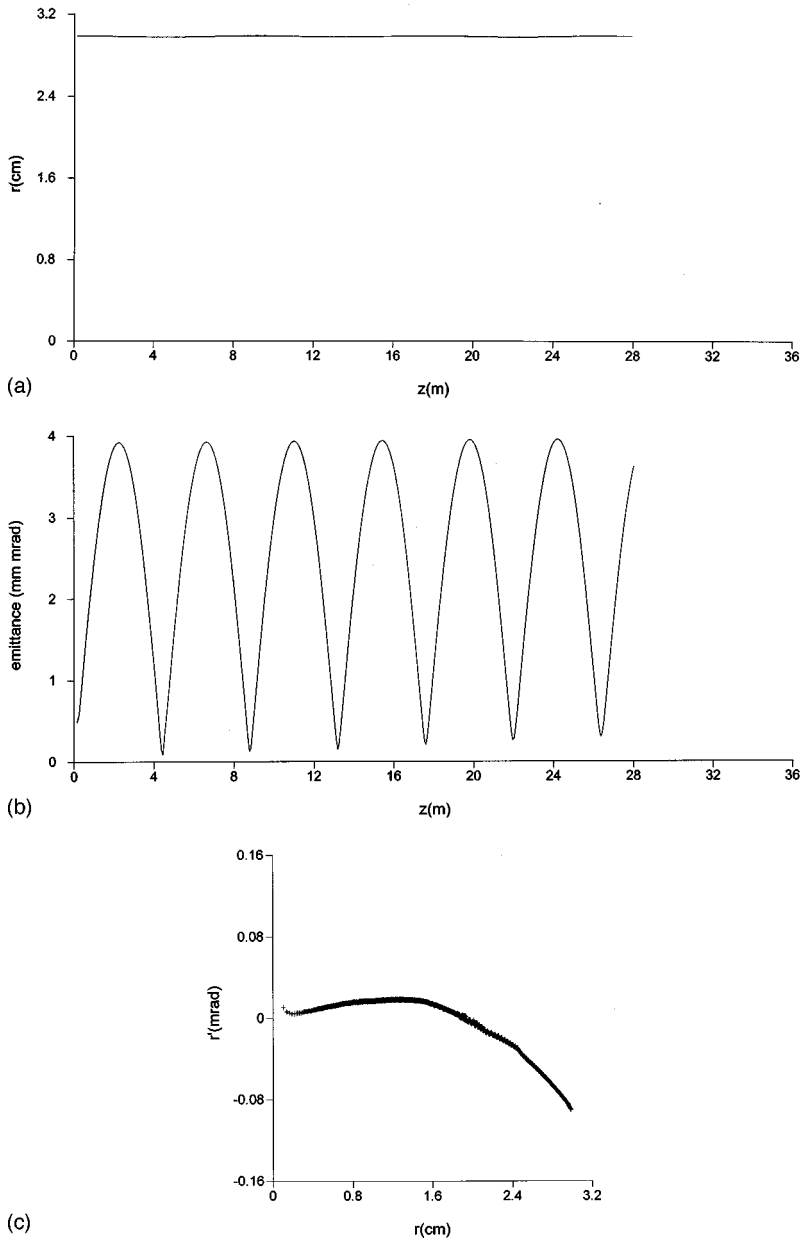

FIG. 1. Numerical results for the balanced flow case. (a) Radial beam profile. (b) Emittance profile, showing correlated oscillations. (c) Final beam phase-space plot, showing differential betatron rotation.

which case the emittance growth is permanent as the beam relaxes to the new stationary state. Also note for the case shown in Fig. 1, there is no nonlinear free energy, and no resulting permanent emittance growth due to an excess of thermodynamic energy.

In Fig. 2 we show simulation results where the beam is mismatched in the uniform-focusing channel, and the Lorentz force equation was modified so effects from energy variations from beam compression and expansion [the third term in the first parentheses in Eq. (18)] were ignored. Note for this case the envelope period is about 5.75 m. The emittance [Fig. 2(b)] still oscillates, but now the oscillation period is a beating between the envelope period and the half-plasma period, and the magnitude of the oscillations increases at an approximate rate of 2 mm mrad per meter. In Fig. 2(c) we see that the emittance growth is still due to a differential rotation in phase space. The emittance oscillations are now driven by variations in the particles' axial velocity in the space-charge force term γ^* in Eq. (18), as the beam compresses and expands. We attribute the increase in the magnitude of the emittance oscillations to a parametric pumping of the differential betatron rotation by the oscillations of the beam core. Although the emittance does vanish at the proper axial locations, this effect may be problematic in actual accelerators, especially if the phase space mixes.

B. Axial velocity variations in a solenoid

Now let us consider the effect from the spread in the axial velocity of the beam within the solenoid. The variation in the axial velocity ($v_z = v_a + v$) is given by

$$v = \frac{\gamma_1}{\gamma_a^3}\frac{c^2}{v_a} - \frac{c^2}{2v_a}\beta_r^2 - \frac{c^2}{2v_a}\beta_\theta^2, \tag{29}$$

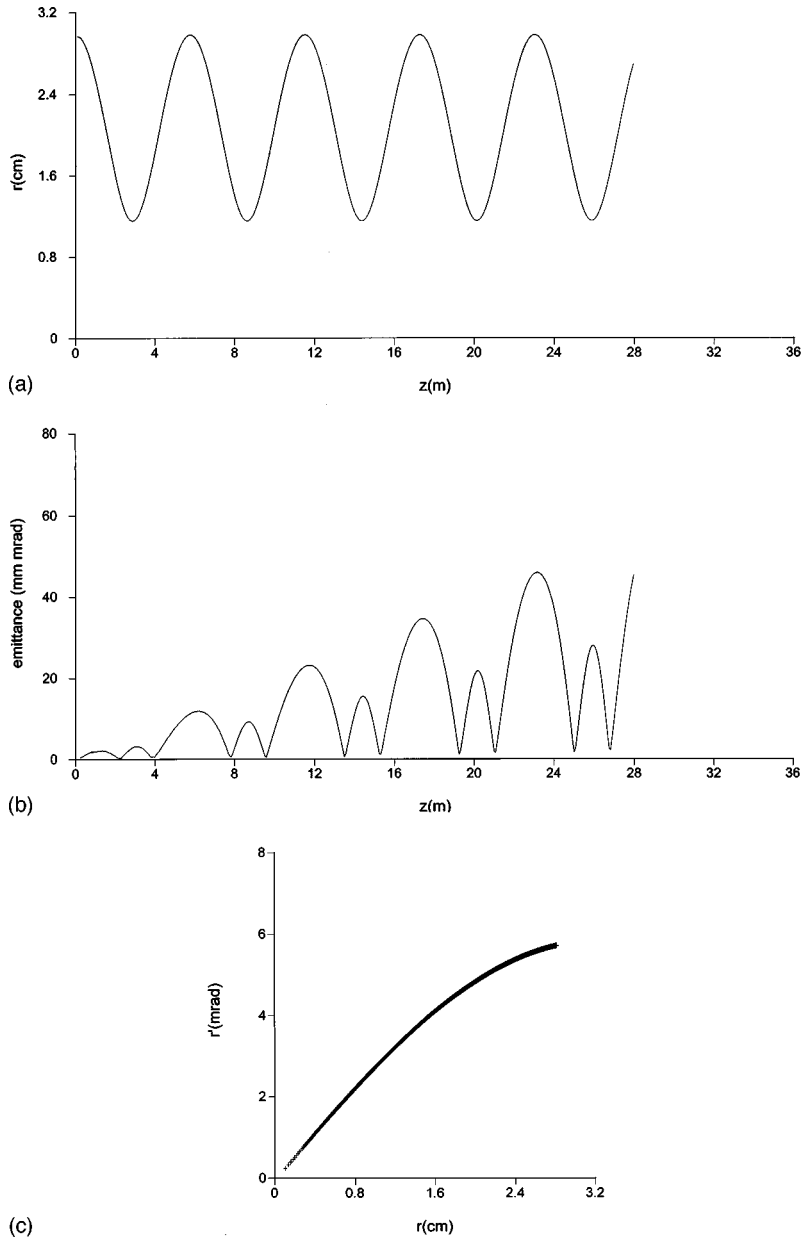

FIG. 2. Mismatched beam with uniform focusing (modified Lorentz force equation ignoring energy variations from beam compression and expansion). (a) Radial beam profile. (b) Emittance profile. (c) Final beam phase-space plot.

where v_a is the axial velocity at the center of the beam. Inside the solenoid, the azimuthal velocity term dominates, and we find

$$v = -\frac{c^2}{2v_a}\beta_\theta^2 = -\frac{e^2B_a^2r^2}{8\gamma_a^2m^2v_a}. \tag{30}$$

This leads to the divergence in the beam introduced by the solenoid (ignoring all terms except for the terms depending on the solenoid's focal length) as

$$\delta r' = -\frac{r}{f}\left(1-2\frac{v}{v_a}\right) = -\frac{r}{f}\left(1-\frac{r^2}{lf}\right). \tag{31}$$

The normalized, 90% emittance growth from the nonlinear part of this divergence is now

$$\varepsilon = \frac{1}{12\sqrt{2}}\,\gamma_a\,\frac{r_b^4}{lf^2}. \tag{32}$$

For the case of the ITS final focus solenoid (solenoid length is about 10 cm, focal length is about 60 cm, and the beam radius is about 3 cm), the emittance growth is about 18 mm mrad. If the beamline consists of several discrete solenoids with the beam being focused tightly between them, the emittance from this effect may or may not accumulate, depending on the relation between the beam's betatron period and the spacing between solenoids. For laminar flow between solenoids, there is also an axial velocity shear, which depends both on the radial divergence of the beam and the potential depression of the beam. If the radial divergence effect dominates, particles at the center of the beam still have a greater axial velocity, and the nonlinearity here will tend to cancel

the nonlinearity induced inside the solenoids. If the beam's potential energy effect dominates, particles at the center of the beam have a smaller axial velocity, and the nonlinearity here will tend to add to the nonlinearity induced inside the solenoids.

C. Gentle scalloping case

In general, the beam is not in completely balanced, uniform flow or being focused hard to a waist. The solenoids are usually discrete, and the beam-edge radius gently undulates down the beamline. Alternatively, we can have scalloping if the beam is mismatched into a uniform-focusing channel. We can estimate the emittance growth for a length l of scalloping motion, by using the divergence term in Eq. (18) while assuming that the beam radius is a constant.

In this case, the accumulated nonlinear divergence after a length l is given by

$$\delta r' = -l\,\frac{eE_r r^2}{\gamma_a m c^2 r_b^2}\,\overline{\alpha^2} = -2\,\frac{Ilr^3}{\gamma_a \beta I_A r_b^4}\,\overline{\alpha^2}, \tag{33}$$

where now $\overline{\alpha}$ is the rms divergence of the scalloping of the radial beam edge. For this case, the normalized, rms emittance growth is given by

$$\varepsilon = \frac{\sqrt{2}}{12}\,l\,\frac{I}{I_A}\,\overline{\alpha^2}, \tag{34}$$

or

$$\varepsilon = \frac{\sqrt{2}}{24}\,l\,\frac{I}{I_A}\,(\delta k_e)^2, \tag{35}$$

if the radial oscillation is sinusoidal, δ is the magnitude of the radial oscillations, and k_e is the envelope oscillation wave number. Note that the beam radius and energy are not present in these equations. For the numbers used in the previous examples with a rms divergence of 20 mrad, the normalized, rms emittance growth is about $1.1(10^{-5})l$, which can become large if this emittance growth is accumulated over a long distance. Note that the worst situation is if the beam flow is laminar, because the particles' phase space is disrupted in the same manner if the beam is converging or diverging. There will also always be an accumulation over a long distance when the beam is in the emittance-dominated regime; but the exact rate depends on the correlation between the particles' betatron period and the period of the scallops.

These expressions can be conveniently approximated for both the cases of a matched beam in a channel of discrete thin solenoids and a mismatched beam in a uniform channel, for modest oscillation magnitudes, using the envelope equation for the beam envelope radius edge r_b [6],

$$r_b'' + k_0^2 r_b - \frac{2K}{r_b} - \frac{4\varepsilon_{\rm un}^2}{r_b^3} = 0, \tag{36}$$

where the unnormalized emittance is defined as $\varepsilon_{\rm un} = \varepsilon/\beta\gamma$ and k_0 is the undepressed betatron wave number. In the limit of laminar flow (vanishing unnormalized emittance $\varepsilon_{\rm un}$), the rms beam divergence for the matched, periodic case with thin solenoids is given by

$$\overline{\alpha^2} = \frac{K^2}{3r_b^2}\,l_s^2, \tag{37}$$

where l_s is the separation between solenoids. For this case, the average rms emittance growth rate is [using Eq. (34)]

$$\frac{\Delta\varepsilon}{\Delta z} \approx \frac{\sqrt{2}}{36}\,\frac{I}{I_A}\,\frac{K^2}{r_b^2}\,l_s^2 = \frac{\sqrt{2}}{9}\left(\frac{I}{I_A}\right)^3 \frac{l_s^2}{r_b^2\gamma^6\beta^6}$$

(matched, periodic focusing). (38)

For the case of a mismatched beam in a uniform focusing channel, we use the envelope equation to find the envelope wave number, $k_e = \sqrt{4K/r_b^2 + 16\varepsilon_{\rm un}^2/r_b^4}$. For the case where the unnormalized emittance is very small (quasilaminar flow), we find [using Eq. (35)]

$$\frac{\Delta\varepsilon}{\Delta z} \approx \frac{\sqrt{2}}{6}\,\frac{I}{I_A}\,\frac{K}{r_b^2}\,\delta^2 = \frac{\sqrt{2}}{3}\left(\frac{I}{I_A}\right)^2 \frac{\delta^2}{r_b^2\gamma^3\beta^3}$$

(mismatch, uniform channel). (39)

It should be remembered that the emittance growths described in Eqs. (38) and (39) are for specific focusing scenarios, which leads to the property that the emittance growth rate decreases with beam energy. Recall from Eq. (34) that the emittance growth rate actually only depends on the beam current and the rms beam convergence or divergence. Equations (38) and (39) are presented for comparison with the emittance growth from the beam's nonlinear free energy and with simulations.

IV. DISCUSSION COMPARING THE MAGNITUDES OF THE GEOMETRICAL EMITTANCE GROWTH AND THE EMITTANCE GROWTH FROM NONLINEAR FREE ENERGY

In this section we compare the magnitude of the predicted emittance growth for a scalloping beam in a uniform focusing channel, using Eq. (39) for the geometrical effect and formulas in [6] for the effect of the nonlinear free-energy effect. We additionally use the simulation code SLICE to numerically calculate the emittance growth for verification of the estimates. There is no nonlinear free energy and hence no thermodynamic emittance growth for a matched beam in a periodic channel, and no comparison is relevant.

Reducing the equations in [6] for the case of a scalloping laminar beam in a uniform channel, we find that the emittance growth (this is the total allowable emittance growth and not a rate) becomes

$$\varepsilon = \frac{\gamma\beta k_0 r_b \delta}{\sqrt{2}}, \tag{40}$$

where, as before, δ is the magnitude of the radial oscillation. For small initial emittances (where the undepressed betatron wavelength is very nearly equal to the square root of two times the generalized perveance divided by the equilibrium beam rms radius), the total emittance growth is approximately

$$\varepsilon \approx \gamma\beta\sqrt{K}\,\delta, \tag{41}$$

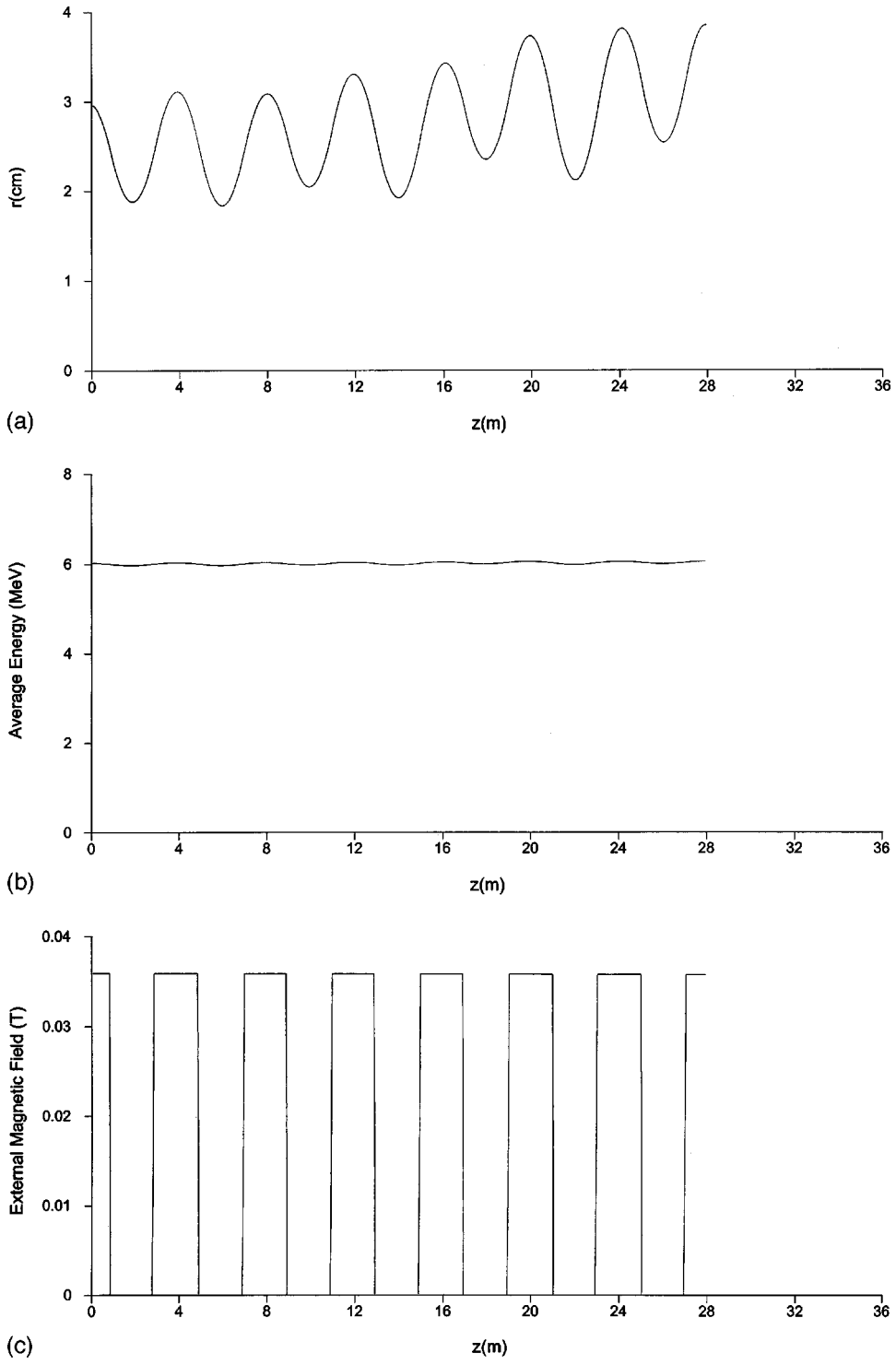

FIG. 3. Periodic focusing case (modified Lorentz force equation ignoring nonlinearities in the space-charge term). (a) Radial beam profile. (b) Average particle kinetic energy profile. (c) Externally applied magnetic field profile. (d) Emittance profile. (e) Final beam phase-space plot. (f) Final beam configuration-space plot.

and the rough initial emittance growth rate [using the depressed betatron wavelength as a rough estimate for the scale required for the generation of the emittance growth in Eq. (36)] is

$$\frac{\Delta\varepsilon}{\Delta z}\approx\sqrt{K}\,\frac{\delta\varepsilon_i}{\pi r_b^2}=\sqrt{\frac{2I}{I_A\gamma^3\beta^3}}\,\frac{\delta\varepsilon_i}{\pi r_b^2}, \tag{42}$$

where now ε_i is the initial normalized, rms emittance.

Comparing Eqs. (39) and (42), we see that the ratio of the geometrical emittance growth rate to the thermodynamic emittance growth rate is $\sqrt{2}\pi\delta(I/I_A)\sqrt{K}/6\varepsilon_i$. The geometrical emittance growth tends to dominate under the conditions of large radial oscillations, low energy, and small initial emittances. For the numerical example used before, the total expected emittance growth from the nonlinear free energy is

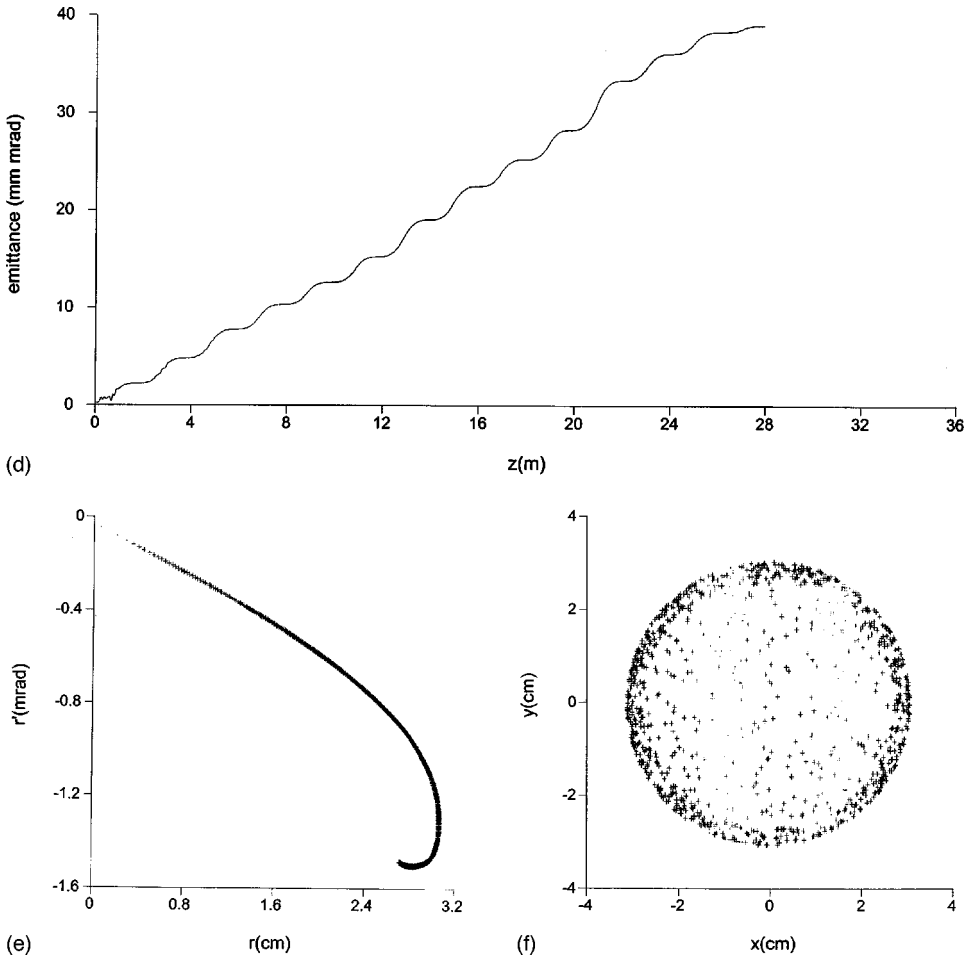

FIG. 3 (*Continued*).

on the order of 1000 mm mrad; however, the geometrical emittance growth rate is about twice the thermodynamic emittance growth rate (for initial emittances of about 30 mm mrad). At lower energies, the geometric effect becomes more dominant—at 3 MeV, the growth rate associated with this effect is about six times as great as the emittance growth from the nonlinear free energy.

In Fig. 3, we show the SLICE outputs for a periodic focusing case. In Fig. 3(a), we see the radial profile, in Fig. 3(b) we see the average particle kinetic energy, in Fig. 3(c) we see the externally applied axial magnetic field, in Fig. 3(d) we see the emittance evolution, in Fig. 3(e) we see the final phase-space plot, and in Fig. 3(f) we see the final configuration-space plot. In this simulation we modified the Lorentz force equation to eliminate the nonlinearity associated with the space-charge term so the effect from the particle energy variations would be very clear. Note the bending back of the beam's phase-space profile, in contrast to that seen in Figs. 1(c) and 2(c), where the emittance is due to only a differential betatron rotation. This deformation of the particles' phase space leads to a hollowing out of the beam's density in configuration space. The average emittance growth rate is about 1.4 mm mrad per meter, in rough agreement with Eq. (38) (which predicts about 2.1 mm mrad per meter). Because we used a nearly matched distribution in the simulation, there is no appreciable emittance growth from any excess nonlinear free energy.

In Fig. 4 we show the SLICE outputs for a mismatched beam in a uniform focusing channel. In Fig. 4(a) we see the radial profile, in Fig. 4(b) we see the average particle kinetic energy, in Fig. 4(c) we see the emittance evolution, and in Fig. 4(d) we see the final phase-space plot. The Lorentz force equation was also modified in this simulation to eliminate the nonlinearity associated with the space-charge term. Again we see the bending back in the beam's phase space, and an average emittance growth of about 1.1 mm mrad per meter, again in rough agreement with that predicted by Eq. (39) (2 mm mrad per meter of drift). For this case, there should also be additional emittance growth from excess nonlinear free energy, and with the parameters used in the simulation, the approximate emittance growth rate from the nonlinear free energy should be of a similar magnitude. However, no thermodynamic emittance growth is observed in the phase-space plot (where it would appear as a broadening of the phase-space distribution instead of a curvature), because it is suppressed by the linearization of the space-charge term.

Of the mechanisms studied in this paper, the effects from beam scalloping will probably dominate in practical beamlines and accelerators, even at high beam energies [remember that in Eq. (34) the emittance growth rate only depends on the beam current and rms divergence, and is independent of the beam energy]. In regards to that mechanism, we can make the following relevant observations.

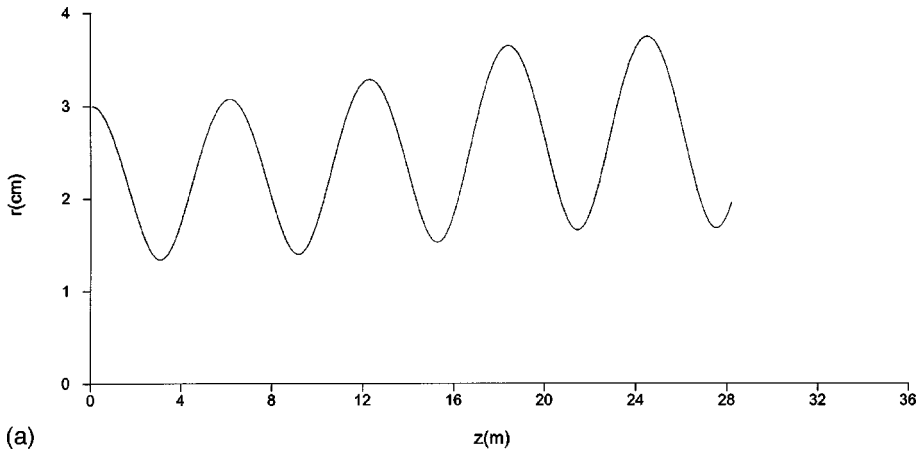

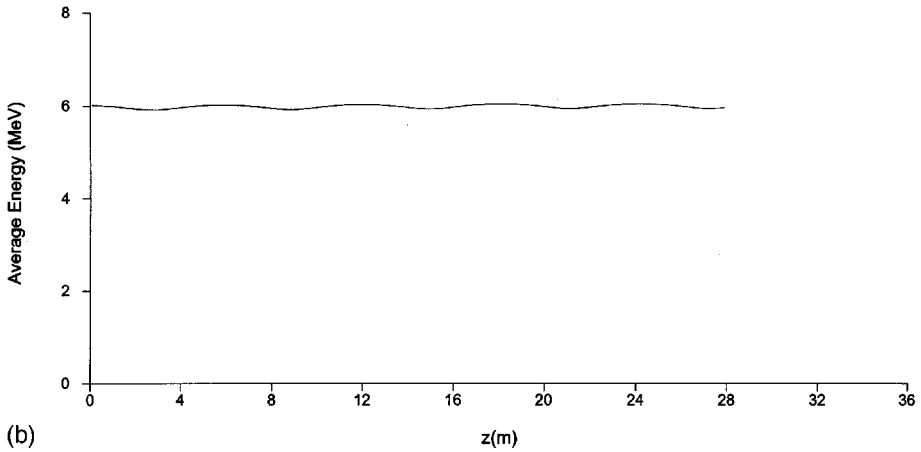

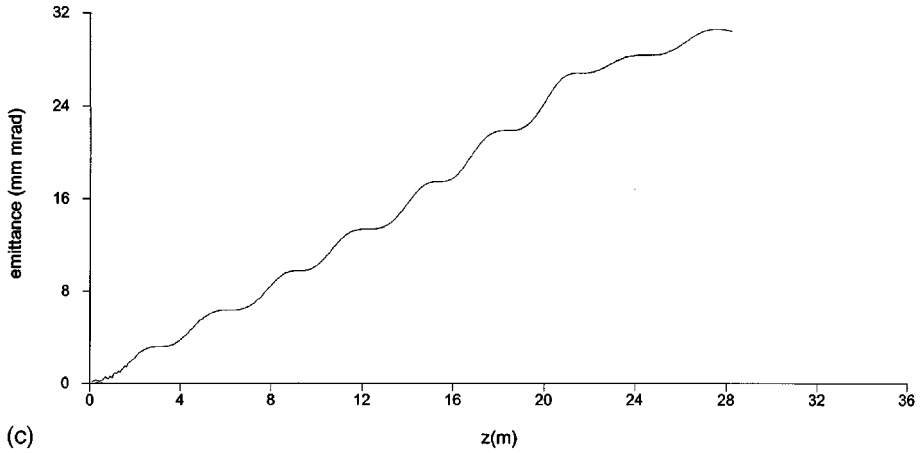

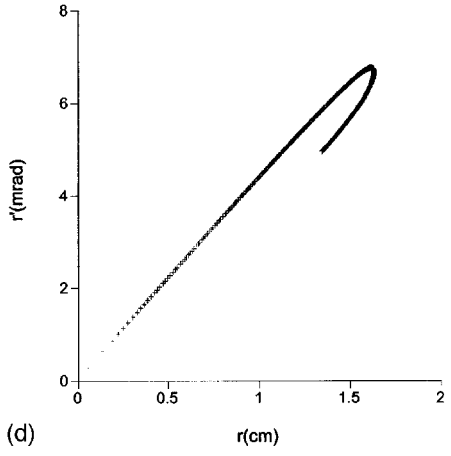

FIG. 4. Mismatched beam with uniform focusing (modified Lorentz force equation ignoring nonlinearities in the space-charge term). (a) Radial beam profile. (b) Average particle kinetic energy profile. (c) Emittance profile. (d) Final beam phase-space plot.

(1) For a mismatch in a uniform channel, the rms emittance as defined in Eq. (1) will grow both from geometric reasons and from thermodynamic reasons. Once a new stationary state is established and the beam is no longer mismatched, both the thermodynamic and geometric emittance growths vanish. The total amount of emittance growth from the nonlinear free energy is predictable from physical arguments [Eqs. (36) and (37)]; the rate of emittance growth from the geometric effects is also [Eqs. (34) and (35)]. Either effect can lead to the largest contribution in the total rms emittance, depending on the depressed betatron period, the beam current, the beam radius, and the beam energy. As a rule, the geometric mechanism will dominate for intense, high-energy, low-emittance beams.

(2) For matched beam oscillations in a periodic focusing channel, the beam is already in a stationary state and there is no excess nonlinear free energy leading to an emittance growth. However, the geometric emittance growth will continue essentially unbounded at the same rate (it will only stop when the energy variations lead to complete betatron mixing which would take a number of depressed betatron periods on the order of the beam energy divided by the change in particles' energies). Since the emittance growth is not tied into a relaxation period of the beam, the total rms emittance growth can become immense. The rate of the emittance growth is just dependent on the beam current and the rms divergence angle of the envelope.

(3) The emittance oscillations that increase in magnitude due to the change in particles' axial velocity as the beam compresses and expands may also become problematic for practical accelerator beamlines.

(4) The hollowing out of the beam [seen in Figs. 3(e), 3(f), and 4(d)] due to these geometric mechanisms can trigger additional emittance growths from both the nonlinear free energy of the nonuniform beam density and also from mechanisms that exist in the emittance-dominated regime [18].

(5) These effects can scale strongly with beam energy [see, for example, Eqs. (38) and (39)]. This leads to a rough quantitative evaluation of how important it is to maintain a high diode voltage, in terms of both the induced emittance growth and the associated distortion in phase space. An injector at half the voltage, but with similar optics, will have well over an order of magnitude more emittance growth and phase-space distortion in the anode magnet capture region, than an injector at full voltage.

ACKNOWLEDGMENTS

This work was supported by funds from the Laboratory-Directed Research and Development program at Los Alamos National Laboratory, which is operated by the University of California for the U.S. Department of Energy. The author is pleased to acknowledge helpful discussions with Simon Yu and Martin Reiser.

[1] Y.-J. Chen, Nucl. Instrum. Methods Phys. Res. A **292**, 455 (1990).
[2] W. C. Turner, S. L. Allen, H. R. Brand, G. J. Caporaso, F. W. Chambers, Y. J. Chen, F. E. Coffield, F. J. Deadrick, T. A. Decker, L. V. Griffith, D. L. Lager, W. J. Mauer, W. E. Nexsen, A. C. Paul, V. L. Renbarger, and S. Sampayan (unpublished).
[3] Y.-J. Chen (unpublished).
[4] D. Kehne, M. Reiser, and H. Rudd (unpublished).
[5] M. Reiser (unpublished).
[6] M. Reiser, *Theory and Design of Charged Particle Beams* (Wiley, New York, 1994), Chap. 6.
[7] P. G. O'Shea (unpublished).
[8] K. J. Kim and R. G. Littlejohn (unpublished).
[9] B. E. Carlsten, Nucl. Instrum. Methods Phys. Res. A **285**, 313 (1989).
[10] B. E. Carlsten, Part. Accel. **49**, 27 (1995).
[11] X. Qui, K. Batchelor, I. Ben-Zvi, and X-J. Wang, Phys. Rev. Lett. **76**, 3723 (1996).
[12] L. Serafini and J. B. Rosenzweig, Phys. Rev. E **55**, 7565 (1997).
[13] D. T. Palmer, X. J. Wang, I. Ben-Zvi, R. H. Miller, and J. Skaritka (unpublished).
[14] K. J. Kim, Nucl. Instrum. Methods Phys. Res. A **275**, 201 (1989).
[15] J. F. Gittens, *Power Travelling-Wave Tubes* (Elsevier, New York, 1965).
[16] B. E. Carlsten, Phys. Rev. E **55**, R4893 (1997).
[17] P. Allison, ''DARHT performance prediction for lower emittance,'' DARHT Report No. Technical Note 42, 1993 (unpublished).
[18] B. E. Carlsten, Phys. Plasmas **5**, 1148 (1998).